MAiNTENANCE
The University of Manchester

Proceedings of 1st International Conference on Maintenance Engineering, IncoME-I 2016
The University of Manchester, UK

Paper No ME2016_1160

A study of two bispectral features from envelope signals for bearing fault diagnosis

Ibrahim Rehab[a], Xiange Tian[a], Niaoqing Hu[b], Tianxiao Yan[c], Ruiliang Zhang[c], Fengshou Gu[a] and Andrew D. Ball[a]

[a]Centre for Efficiency and Performance Engineering, University of Huddersfield, Queensgate, Huddersfield, HD1 3DH, UK.

[b]School of Mechatronics and Automation, National University of Defense Technology, Hunan, China, 410073.

[c]School of Mechanical Engineering, Taiyuan University of Technology, Shanxi, China, 030024.

Email: Ibrahim.rehab@hud.ac.uk, u1178848@hud.ac.uk, F.Gu@hud.ac.uk, a.ball@hud.ac.uk

Abstract: To accurately detect and diagnose bearing faults, bispectral analysis has received more attention recently because of its unique property of noise reduction and nonlinearity extraction. Particularly this study investigates two typical bispectra: conventional bispectrum (CB) and modulation signal bispectrum (MSB) for suppressing noise influences in envelope signals and hence obtaining more accurate diagnostic features. The first component from the diagonal slice of CB results and that of the subdiagonal slices of MSB results are taken as the diagnostic features considering effective inclusion of information and easy of computations. Simulative and experimental studies show that both MSB and CB features result in good diagnostic performances but MSB may outperform CB slightly in that it shows smaller variance in attaining the feature and more sensitive to weak fault signatures. This merit of MSB may be due to that the MSB feature has more diagnostic information as it is the combination of first three harmonics, whereas the CB feature is combined from just the first two harmonics.

Keywords: Modulation signal bispectrum, taper roller bearing, fatigue test, condition monitoring, high order statistics.

1.0 Introduction

For an accurate diagnosis of the bearing fault, a number of techniques have been proposed to separate deterministic fault components from noisy bearing vibration. McFadden and Smith [2] reported that the envelope spectrum contain single, discrete components only in the very simplest examples of an axial bearing or a radial bearing with a defect in outer race and it is possible to detect the bearing condition. Randall [3] noted that the discrete random separation (DRS) technique is more successful in separating gear signals from the cyclostationary bearing signals compared to the self-adaptive noise cancellation (SANC) technique. Minimum entropy deconvolution (MED) was first proposed by Wiggins [4] to sharpen the reflections from different subterranean layers in seismic analysis. Spectral kurtosis (SK) provides a means of determining which frequency bands contain a signal of maximum impulsivity. It was first used in the 1980s for detecting impulsive events in sonar signals [5]. Sawalhi et

al. [6] proposed an algorithm using a combination of autoregressive model and MED technique to enhance the defect recognition capability of the SK by sharpening the impulses originating from the defective bearings. However, in these studies, the authors have focused more on tracking the variations of vibration components at the characteristic fault frequency but with limited concentration on noise reduction and utilizing the modulation characteristics in extracting the diagnostic information. Rehab et al [7] applied MSB to extract the fault feature from envelope signals due to its capability to suppress noise for reliable bearing fault severity diagnosis. Tian et al [8] presented a unique method for diagnosing combination faults in planetary gearboxes using a modulation signal bispectrum based sideband estimator (MSB-SE). Furthermore, the authors [9] also proposed a robust MSB detector that allows the achievement of both optimal band selection and envelope analysis, which overcome the filter band optimisation problem in traditional narrowband envelope analysis, compared with optimal envelope analysis using fast Kurtogram.
The purpose of this paper is to accurately estimate the performance of high order spectrum analysis, power spectrum, conventional bispectrum and modulation signal bispectrum based on statistical significance of the estimated spectra in two selected case studies: a simulated time signal where spectral contents is known an then estimate the high order statistics amplitude using Mote Carlo estimator. In the next section vibration signal of taper roller bearing fatigue test were analyzed using aforementioned methods.

2.0 Rolling element bearing vibration signal.

Generally, the vibration signal $x(t)$ from a rolling element bearing with a single-point fault is expressed as [10].

$$x(t) = x_f(t).x_q(t).x_{bs}(t) + x_s(t) + n(t) \quad (1)$$

where $x_f(t)$ is the basic impulse series produced by the fault which impacts repetitiously with another surface in the bearing $x_q(t)$ is the modulation effect due to non-uniform load distribution of the bearings and the cyclic variation of transmission path between the fault impact site and the transducer, and $x_{bs}(t)$ is the bearing induced vibrations. This modulating effect is caused partly by the bearing geometry, but more significantly by the position of the vibration sensor relative to the fault location. It is this element which, if not taken into account\, significantly affects the efficacy of the signal model in real-life situations where optimal sensor position is not possible or perhaps undesirable. $x_s(t)$ is the machinery induced vibration. The signal $x_s(t)$ is an unwanted, structured, and predictable damped harmonic signal which is also considered to be a source of noise. $n(t)$ is a Gaussian white noise sequence with variance σ_n^2. This is unpredictable measurement noise present in any practical measurement system

3.0 Signal processing based on MSB

3.1 Power Spectrum (PS)

The discrete Fourier transform (DFT) $X(f)$ of a discrete time vibration signal $x(t)$, is defined as [11]:

$$X(f) = DFT[x(t)] = \sum_{t=-\infty}^{\infty} x(t)e^{-j2\pi ft} \tag{2}$$

The power spectrum method is generally used to describe the power distribution of signal in the frequency domain. In the same environment, the amplitude of PS increases with the growth of fault severity. So it is widely applied for fault severity diagnosis. Usually it is calculated using Fourier transform (FT) by:

$$p(f) = E\left\langle X(f)X^*(f)\right\rangle \tag{3}$$

where, $X(f)$ and its conjugate $X^*(f)$ are the Fourier Transform of the sequence $x(n)$, and $E\langle.\rangle$ is the expectation operation [12].

3.2 Conventional bispectrum (CB)

Form DFT the conventional bispectrum $B(f_c, f_x)$ can be defined in frequency domain as [13]

$$B(f_c, f_x) = E\left\langle X(f_c)X(f_x)X^*(f_c + f_x)\right\rangle \tag{4}$$

where, $X^*(f)$ is the complex conjugate of $X(f)$ and $E\langle.\rangle$ is the statistical expectation operation. f_c, f_x and $f_c + f_x$ indicates three individual frequency components achieved from Fourier series integral.

On the other hand, if the three spectral components: f_c, f_x and $f_c + f_x$ are nonlinearly coupled to each other, the total phase of the three components will not be random at all, even though each of the individual phases are random, in particular, the phases have the following relationship:

$$\varphi(f_c) + \varphi(f_x) = \varphi(f_c + f_x) \tag{5}$$

Consequently, the statistical averaging will not lead to a zero value in the bispectrum. This nonlinear coupling is indicated by a peak in the bispectrum at the bifrequency $B(f_c, f_x)$. To measure the degree of coupling between coupled components, a normalised form of the bispectrum or bicoherence is usually used and defined as.

$$b^{SE}(f_c, f_x) = \frac{\left|B(f_c, f_x)\right|^2}{E\left\langle\left|X(f_c)X(f_x)\right|^2\right\rangle E\left\langle\left|X(f_c + f_x)\right|^2\right\rangle} \tag{6}$$

The bicoherence is independent of the amplitude of the triple product of the DFT amplitudes and its values are bounded between 0 and 1. The bicoherence is close to 1 if there are nonlinear interactions among frequency combinations, f_c, f_x and $f_c + f_x$. On the other hand, a value of near 0 implies an absence of interactions between the components. The possible amplitudes in the latter case may suggest that the

components are originated independently from a system. Therefore, based on the amplitude of bicoherence the nonlinear interactions can be detected and the interaction degrees can be also measured between the coupling components.

3.3 Modulation signal bispectrum (MSB)

MSB has the capability to detect nonlinear components and suppress random noise by detecting phase coupling in modulation signal. The definition of MSB can be described by Equation (7). [12, 14]

$$B_{MS}(f_c, f_x) = E\left\langle X(f_c + f_x)X(f_c - f_x)X^*(f_c)X^*(f_c)\right\rangle \tag{7}$$

where, $X^*(f)$ is the complex conjugate of $X(f)$ and $E\langle.\rangle$ is the statistical expectation operation. f_c, f_x and $f_c + f_x$ indicates three individual frequency components achieved from Fourier series integral. The magnitude and phase of MSB can be expressed as Equations (8) and (9).

$$A_{MS}(f_c, f_x) = E\left\langle \left|X(f_c + f_x)\right|\left|X(f_c - f_x)\right|\left|X^*(f_c)\right|\left|X^*(f_c)\right|\right\rangle \tag{8}$$

$$\varphi_{MS}(f_c, f_x) = \varphi(f_c + f_x) + \varphi(f_c - f_x) - \left|\varphi(f_c)\right| - \left|\varphi(f_c)\right| \tag{9}$$

It takes into account both $(f_c - f_x)$ and $(f_c + f_x)$ simultaneously in Equation (8) for measuring the nonlinear effects of modulation signals. If $(f_c - f_x)$ and $(f_c + f_x)$ are both due to the nonlinear effect between $(f_c - f_x)$ and $(f_c + f_x)$, there will be a bispectral peak at bifrequency $B_{MS}(f_c, f_x)$. On the other hand, if these components are not coupled but have random distribution the magnitude of MSB will be close to nil. In this way it allows the wideband noise in bearing vibration signals to be suppressed effectively so that the discrete components can be obtained more accurately.
To measure the degree of coupling between three components, a Modulation Signal Bicoherence (MSBc) can be used and calculated by Equation (10).

$$b_{MS}^{SE}(f_c, f_x) = \frac{\left|B_{MS}(f_c, f_x)\right|^2}{E\left\langle \left|X(f_c)X(f_c)X^*(f_c)X^*(f_c)\right|^2\right\rangle E\left\langle \left|X(f_c + f_x)X(f_c - f_x)\right|^2\right\rangle} \tag{10}$$

Based on MSB property of highlighting modulation effect, a MSB detector can be developed. Firstly, MSB amplitude array is averaged along the f_x direction according to Equation (11) to obtain an average spectrum at different f_c.

$$A_j = \frac{1}{N}\sum_i A_{ij} \tag{11}$$

where i and j is the index of f_x and f_c respectively. Then the carrier frequencies which have high amplitudes are selected as the candidates for feature extraction. Finally, the selected f_c slices are farther averaged to get the MSB detector as expressed by Equation (12).

$$MSBdt = \frac{1}{m}\sum_{j=k_1}^{K_m} A_{ij} \tag{12}$$

where $j = k_1, ...k_m$ is the slice number that selected for calculating MSB detector.

4.0 Simulation Study

To evaluate the performance of MSB, CB and PS, in estimating the signal components contaminated with high level of white noise, a harmonic signal was generated with three components at frequencies of 20Hz, 40HZ and 60Hz, pulsing a white noise for a SNR as low as -5dB. Figure 1 shows the results of MSB and CB for the simulated signal. It can be seen that the MSB results have a clear distinct peak at the bifrequency $B_{MS}(f_F, 2f_F)$, while the CB results also show a clear distinct peak at bifrequency $B_{MS}(f_F, f_F)$. Moreover, PS showed a clear peak at $B_{MS}(0, f_F)$.

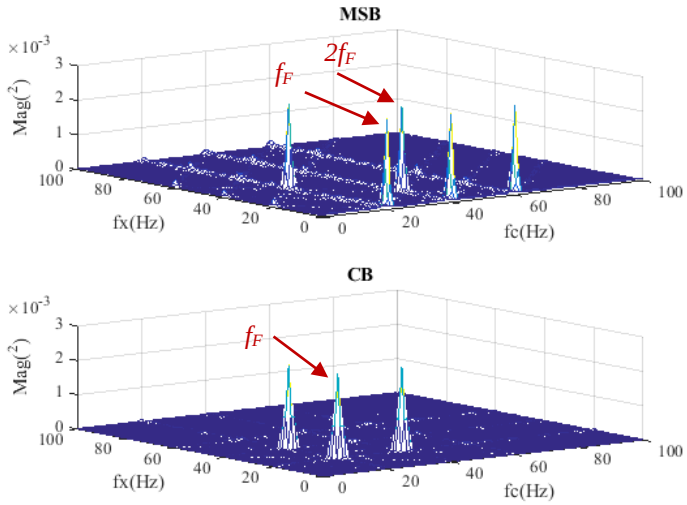

Figure 1. MSB and CB of simulated signals

Twenty Monte Carlo tests were performed, with the feature magnitude with averages being calculated for PS, CB and MSB along the diagonal slices. The signal features were hence extracts using the following magnitude features respectively.

$$D_{PS} = |B_{MS}(0, f_F)|^{4/2} |B_{MS}(0, 2f_F)|^{4/2} \quad (13)$$

$$D_{CB} = |B_{MS}(f_F, f_F)|^{3/2} \quad (14)$$

$$D_{MSB} = |B_{MS}(f_F, 2f_F)|^{4/2} \quad (15)$$

where f_F is the characteristic frequency. These components are usually more significant in an envelope signal and provide sufficient diagnostic information for both the fault components and their severity. Figure 2 illustrates the feature harmonic magnitude of the aforementioned simulated signal. Averages of PS, CB and MSB are shown in blue dotted lines, while the expected magnitude is represented by solid red line. The error has been calculated based on of the different between the mean value of each harmonics magnitude and the expected value. The MSB results exhibit a lower deviation relative to the CB and PS results.

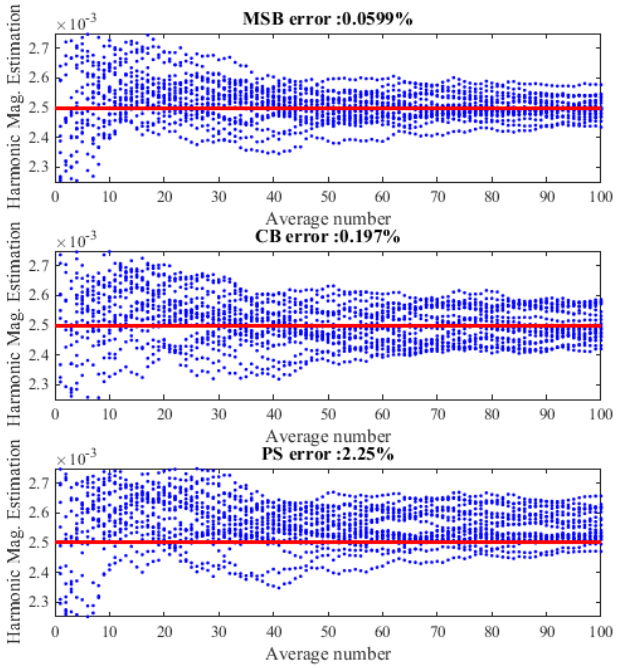

Figure 2. Feature magnitude from Monte Carlo Tests, with Averages

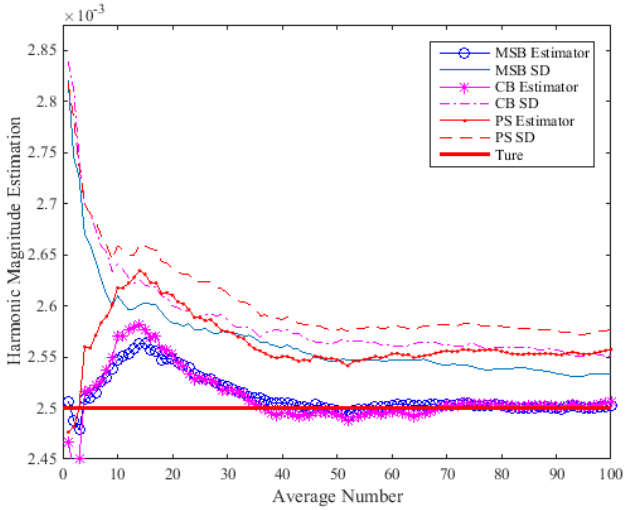

Figure 3. Estimation of variability vs averages

To evaluate the variability of the averaged tests, the average values of MSB, CB and PS were considered as an estimator while the standard deviations were calculated based on the calculated and expected value of the simulated signal. Figure 3 illustrates the estimation of variability in the averages of MSB, CB and PS results. The MSB

method presents a clearer convergence than CB and PS for both the Estimator and the SD calculation

5.0 Experimental verification

5.1 Test rig facility and test procedure

Bearing vibration data was collected from an in house gearbox test rig as shown in Figure 5 (a). The maximum torque of gearbox was 1372 Nm, the rotational speed of the large gear was 1122 rpm and the pinion gear speed was 1400 rpm. Figure 4 (b) shows the position of bearing studied in this experiment. It was mounted on the pinion gear whose rotation frequency is 23.33Hz. An accelerometer mounted in the outer surface of the gearbox on the vertical direction.

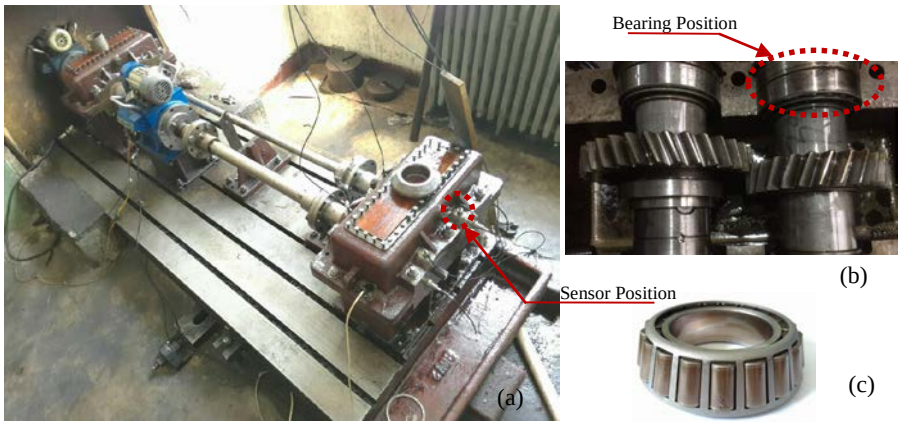

Figure 4. Experimental set-up, (a) test rig components, (b) bearing position and (c) bearing type

In the experiment, the gearbox operated at a constant speed and under constant load conditions. The vibration was measured by a general purpose accelerometer with a sensitivity of 31.9 mv/(m/s^2) and a frequency response range of 1Hz to 10kHz. All the data were logged by a multiple-channel, high-speed data acquisition system at a sampling rate 25.6 kHz and 16-bit resolution. The geometric dimensions of the tapered roller bearings are listed in Table 1, while the bearing defect frequencies are given in and Table 2.

Table 1. Specification of tapered roller bearing type 32212

Parameter	Measurement
Outer diameter	110 mm
Inner diameter	60 mm
Pitch diameter	85 mm
Roller diameter	13 mm
Roller number	19
Contact Angle	14.931^o

Table 2. Fault characteristic frequencies

Fault type	Defect frequency (Hz)
Inner race	254.39
Outer race	188.88
Rolling element	74.61
Cage	9.94

The tests were carried out for 11h13min, at the beginning the data were collected once every 9min and data duration of 1min. during the test an abnormal sound appeared at 60 time index of the data collection then the data collection intervals have been reduced to 4min. during the test the RMS and kurtosis have calculated to monitor the change of the vibration signal.

badly fatigued inner race

one rolling element has a fatigue dent

little scratched outer race

Figure 5. Photographs of Bearing Faults

6.0 Signal processing results and discussion

6.1 Online results

Figure 6 shows the RMS and kurtosis of the collected data, which were obtained online. the RMS values increse gradually for the initial 50 test time index they then increase rapidly as a result of incresing surface fatigue leading to increased vibraion. The kurtosis values increase gradually for the first 60 test time index and then more rapidly up to 72 test time index. Beyond this the kurtosis decreases as result of the increse the fatigue surface. At that point the test was stopped because of the high levels of vibration. Subsquent offline inspection indicated that the bearing was havily damaged as show in Figure 5.

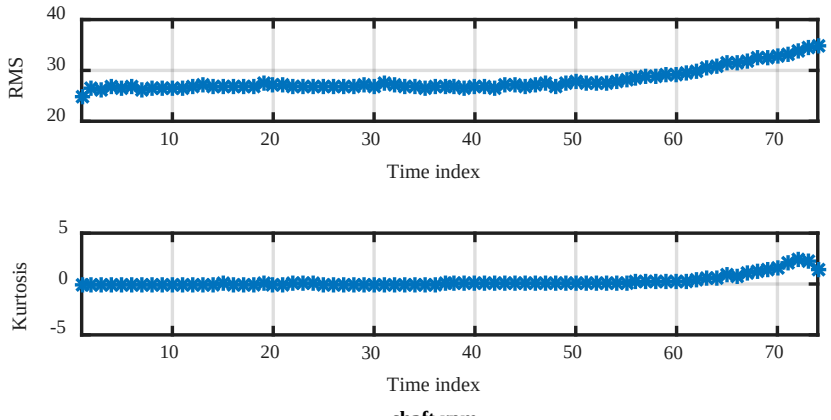

Figure 6. RMS and Kurtosis of the collected data

6.2 MSB and CB results

To investigate the early signs of bearing defects and to evaluate the performance of the two bispecta analysis techniques, a vibration signal processing procedure was employed. This is illustrated in Figure 7. Firstly, the envelope of vibration signal was calculated. Then, CB and MSB analysis were carried out to enhance the nonlinear components in the envelope signal. The next step was to extrac the features using the first component from the diagonal slice of CB results and that of the sub-diagonal slices of MSB results. Finally, the fault type and severity were examined using the these features.

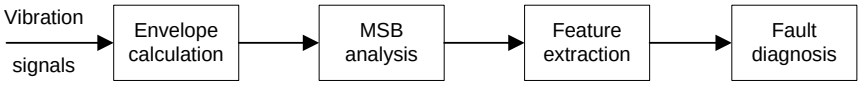

Figure 7. Signal processing procedure

The MSB and CB results from the bearing's vibration signal at time index 1 are illustrated in Figure 8. It can be seen that at the beginning of the test the bearing has a fault on both the inner race and the cage. The signal magnitude at the inner race fault frequency f_i is clearly visible using MSB, as well as the both sidebands, but nothing can be seen from CB. For the cage defect the second harmonic of the cage frequency $2 * f_c$ is clearly visible from both MSB and CB, with CB producing the higher magnitude.

Figure 9 shows the MSB and CB analysis of the bearing vibration data for test time index 74. Increased magnitude of inner race fault and cage fault can be seen in comparasion with Figure 8 based on the MSB detector. Meanwhile, for the CB detector the magnitude of the cage defect at the second harmonic is close to that observed in Figure 8. Moreover, the magnitude of the inner race defect appears to be high when

using CB detector. Thus, the MSB exhibits a good noise reduction performance and can therefore be used to identify the fault type more accurately than CB.

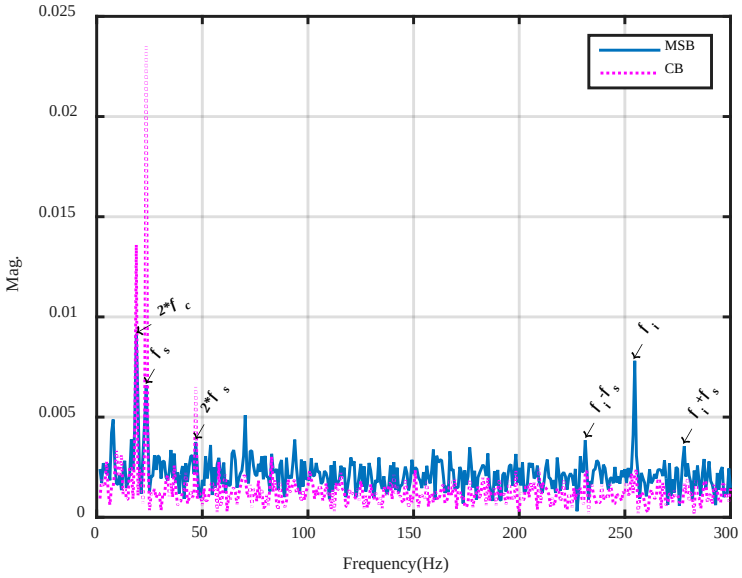

Figure 8. MSB and CB of the time index 1

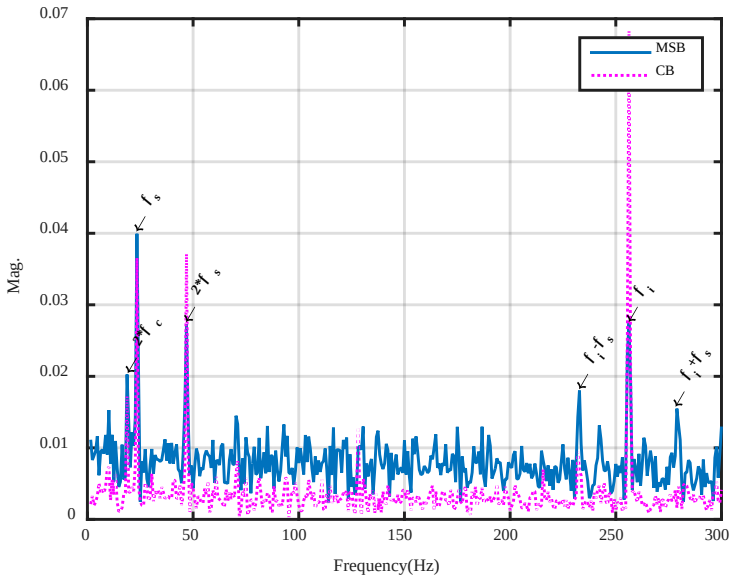

Figure 9. MSB and CB of the time index 74

7.0 Conclusion

The study shows that CM and MSB allows significant suppression of noise content in a envelope signal and leads to more accurate diagnostic features. In particular, the CB and MCB directly combine the magnitude information of the first a few harmonics which are usually more significant in an envelope signal and provide sufficient diagnostic information for both the fault components and severity.
Monte Carlo tests show that the MSB features exhibit less deviation and lower variation between different tests, compared with that of PS and CB, showing that MSB performs better in extracting the diagnostic information as its first component combines the first three harmonics in the original spectrum and has higher SNR compared with that from CB and PS which includes only the first two harmonics. As a results MSB provide more sensitive detection of the incipient faults occurring the tapper bearing of the gearbox.

References

1. Craig, M., et al., *Advanced condition monitoring of tapered roller bearings, Part 1*. Tribology International, 2009. 42(11–12): p. 1846-1856.
2. McFadden, P. and J. Smith, *Model for the vibration produced by a single point defect in a rolling element bearing.* Journal of Sound and Vibration, 1984. 96(1): p. 69-82.
3. Randall, R.B., *Detection and diagnosis of incipient bearing failure in helicopter gearboxes.* Engineering Failure Analysis, 2004. 11(2): p. 177-190.
4. Wiggins, R.A., *Minimum entropy deconvolution.* Geoexploration, 1978. 16(1): p. 21-35.
5. Dwyer, R.F. *Detection of non-Gaussian signals by frequency domain kurtosis estimation*. in *Acoustics, Speech, and Signal Processing, IEEE International Conference on ICASSP'83*. 1983. IEEE.
6. Sawalhi, N., R.B. Randall, and H. Endo, *The enhancement of fault detection and diagnosis in rolling element bearings using minimum entropy deconvolution combined with spectral kurtosis.* Mechanical Systems and Signal Processing, 2007. 21(6): p. 2616-2633.
7. Rehab, I., et al., *The fault detection and severity diagnosis of rolling element bearings using modulation signal bispectrum.* 2014.
8. Tian, X., et al. *Diagnosis of combination faults in a planetary gearbox using a modulation signal bispectrum based sideband estimator*. in *Automation and Computing (ICAC), 2015 21st International Conference on*. 2015. IEEE.
9. Tian, X., et al., *A robust fault detection method of rolling bearings using modulation signal bispectrum analysis*, in *28th International Congress of Condition Monitoring and Diagnostic Engineering Management (COMADEM 2015)*. 2015: Buenos Aires, Argentina p. 1-7.

10. Kıral, Z. and H. Karagülle, *Vibration analysis of rolling element bearings with various defects under the action of an unbalanced force.* Mechanical Systems and Signal Processing, 2006. **20**(8): p. 1967-1991.
11. Xinxin, L., et al. *Feature Extraction of Underwater Signals Based on Bispectrum Estimation*. in *Wireless Communications, Networking and Mobile Computing (WiCOM), 2011 7th International Conference on*. 2011. IEEE.
12. Alwodai, A., et al., *A Study of Motor Bearing Fault Diagnosis using Modulation Signal Bispectrum Analysis of Motor Current Signals.* Journal of Signal and Information Processing, 2013. **4**: p. 72.
13. Kim, Y.C. and E.J. Powers, *Digital Bispectral Analysis and Its Applications to Nonlinear Wave Interactions.* Plasma Science, IEEE Transactions on, 1979. **7**(2): p. 120-131.
14. Gu, F., et al., *Electrical motor current signal analysis using a modified bispectrum for fault diagnosis of downstream mechanical equipment.* Mechanical Systems and Signal Processing, 2011. **25**(1): p. 360-372.

Authors' Biography

	**Ibrahim Rehab** Ibrahim is from Libya. He was an engineer at the General Electric Company of Libya at the general projects department of the power generation. Ibrahim started his PhD research program on the 1st of October 2010 as full time student, his project title is the optimization of vibration data analysis for the detection and diagnosis of incipient faults in roller bearings.
	**Xiange Tian** Xiange, originally from China, got the bachelor's and master's degree in Shandong University of Science and Technology and major in Electronic Information Engineering and Signal & Information Processing, respectively.
	**Fengshou Gu** Dr Fengshou Gu is one of our experts in the fields of vibro-acoustics analysis and machinery diagnosis, with over 20 years of research experience. He is the author of over 100 technical and professional publications in machine dynamics, signal processing, condition monitoring and related fields.
	**Andrew D. Ball** Professor Andrew's personal research expertise is in the detection and diagnosis of faults in mechanical, electrical and electro-hydraulic machines, in data analysis and signal processing, and in measurement systems and sensor development. He is the author of over 250 technical and professional publications, and he has spent a large amount of time lecturing and consulting to industry in all parts of the world.